sciendo

DOI 10. 2478/ama-2022-0047

acta mechanica et automatica, vol.16 no.4 (2022)

APPLICATION OF THE DEFORMATION FRACTURE CRITERION TO CRACKING OF DISC SPECIMENS WITH A CENTRAL NARROW SLOT

Andrzej KAZBERUK*

*Faculty of Mechanical Engineering, Bialystok University of Technology, ul. Wiejska 45C, 15-351 Bialystok, Poland

a.kazberuk@b.edu.pl

received 9 October 2022, revised 20 October 2022, accepted 20 October 2022

Abstract: Using the method of singular integral equations, the elastic-plastic problem for cracked Brazilian disk was solved. Based on the Dugdale model and deformation fracture criterion, the relationships between critical load, notch tip opening displacement and length of the plastic strips were established. Also, the comparison between the present solution for the finite domain and the known solution obtained for the semi-infinite notch in the elastic plane was performed.

Key words: cracked Brazilian disc, Dugdale model, plastic strips, fracture deformation criterion, singular integral equations

1. INTRODUCTION

The application of the deformation fracture criterion in determining the basic fracture mechanics parameters requires the knowledge of the relationship between the load level and the opening displacement at the crack tip. This means that for an arbitrary test element, not only the stress field should be determined, but also the strain field considering the changes taking place in the fracture process zone. The general solutions for a crack or notch in the infinite plane are known ([1], see also the literature [2]) but for a particular specimen, these solutions can be only regarded as asymptotic. This work aims to determine the relationship between the load level and the opening displacement at the notch tip for a cylindrical specimen with a central narrow slot.

The Brazilian test is a simple indirect testing method, which is used to obtain the tensile strength of brittle materials such as concrete, rock, and rock-like materials. An up-to-date review of works concerning various aspects of the Brazilian test can be find in the literature [3,4].

A disc with an internal central crack as a convenient experimental specimen was considered analytically by [5–9]. These results concerning stress field distribution and values of the stress intensity factors were confirmed by Atkinsons et al. [10] and Awaji and Sato [11]. Recent works devoted to the investigation of the fracture process in quasi-brittle materials using a compressed disc with a central slot are [12–21].

The basic material parameter in fracture mechanics is the critical stress intensity factor determined experimentally on specimens with initial cracks. In the case of metals, the procedure for determining this parameter is standardised and widely used. The fracture process in this case begins with the fatigue-initiated crack. For quasi-brittle materials such as concrete, ceramics or rocks, it is difficult to obtain an initial crack with strictly defined parameters. Usually, the initial crack is produced at the specimen forming stage. In this way, slots of quite significant (2–4 mm) width and rounded tips are obtained. Also, previously cited sources devoted to analytical investigation of stress concentration in disc specimens refer to strict mathematical crack, i.e. the crack of zero width.

The method of determining the critical stress intensity factor of a quasi-brittle material on a compressed disc specimen with a centrally located narrow slot is presented. Knowing the value of the critical load and standard material constants, the critical stress intensity factor is calculated using the deformation fracture criterion [22] based on the Dugdale model [23,24]. The results were compared to previously published approximate relationships for semi-infinite U-notch in an elastic-plastic plate subjected to tension [25].

2. PROBLEM FORMULATION

There are two equal ($\mathrm{l}_2 = \mathrm{l}_3 = \ell$) linear cuts (contours L_2 and L_3) emanating from the slot vertices and placed on the axis Ox. These cuts will model the fracture process zone as plastic strips 26]. We assume that that Tresca-Saint Venant plasticity condition is fulfilled in these bands. The overall unknown relative extent of all defects weakening disc specimen we define as $\gamma = (\ell_0 + \ell)/\mathrm{R}$.

The set of dimensionless geometric parameters (ε_0, γ_0 γ) fully describes the domain under consideration. Assuming radius R as the basic unit length, we obtain relationships

$$\ell_0 = \gamma_0 R, \quad \ell = (\gamma - \gamma_0) R, \quad \rho = \varepsilon_0 \gamma_0 R. \tag{1}$$

Suppose that the hole edge (the smooth contour L_1) is free of applied loads. The disc is loaded by two concentrated forces P, which compress the specimen along the Ox axis (Fig.1). Such type of loading causes the concentration of tensile stresses invertices ($\pm\ell_0$) of the hole.

The problem will be solved using the singular integral equation method [27] (see also Savruk and Kazberuk [2]). Complex stress potentials are written in the form [27]

DOI 10.2478/ama-2022-0047

$$\Phi_*(z) = \Phi_0(z) + \Phi(z), \quad \Psi_*(z) = \Psi_0(z) + \Psi(z), \tag{2}$$

where functions [28]:

$$\Phi_0(z) = \sigma_p \frac{z^2+R^2}{2(z^2-R^2)}, \qquad \Psi_0(z) = \sigma_p \frac{2R^4}{(z^2-R^2)^2}. \tag{3}$$

Nominal stress $\sigma_p = P/(\pi R)$ is equal to normal stress σ_y alongside Ox axis, $z = x + iy$.

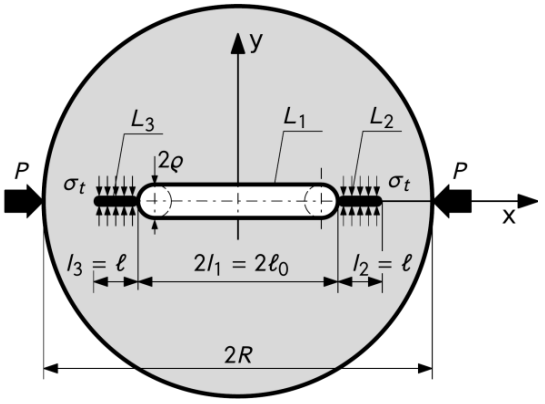

Fig. 1. Disc specimen weakened by central narrow slot and plastic strips subjected to compression by concentrated forces

Functions $\Phi_0(z)$, $\Psi_0(z)$ describe the stress state in the solid disc (i.e. without a hole) loaded by concentrated forces, whereas potentials $\Phi(z)$, $\Psi(z)$ characterise the disturbed stress state induced by the opening (L_1) and cuts (L_2, L_3). These potentials are written in the following form [27]:

$$\Phi(z) = \frac{1}{2\pi}\int_L \left\{\left[\frac{1}{t-z} + \frac{\bar{t}}{z\bar{t}-R^2}\right] g'(t)\,dt + \frac{z(t\bar{t}-R^2)(z\bar{t}-2R^2)}{R^2(z\bar{t}-R^2)^2}\overline{g'(t)}\,d\bar{t}\right\}, \tag{4}$$

$$\Psi(z) = \frac{1}{2\pi}\int_L \left\{\left[\frac{\bar{t}^3}{(z\bar{t}-R^2)^2} - \frac{\bar{t}}{(t-z)^2}\right] g'(t)\,dt + \left[\frac{1}{t-z} + \frac{\bar{t}}{z\bar{t}-R^2} + \frac{\bar{t}(z\bar{t}-3R^2)(t\bar{t}-R^2)}{(z\bar{t}-R^2)^3}\right]\overline{g'(t)}\,d\bar{t}\right\}.$$

Here $g'(t)$ $(t \in L_k,\ k = 1,2,3)$ is an unknown function of the derivative of displacement discontinuity vector across the cut contour.

The boundary condition at the contour L has the following form:

$$N(t) + iT(t) = p(t) \quad t \in L, \quad L = \bigcup_{k=1}^{3} L_k, \tag{5}$$

where N and T are normal and tangential components of the stress vector. The right side of the Eq. (5) is equal [27]:

$$p(t) = \sigma_k - \left\{\Phi_0(t) + \overline{\Phi_0(t)} + \frac{d\bar{t}}{dt}\left[t\overline{\Phi_0'(t)} + \overline{\Psi_0(t)}\right]\right\}, \quad t \in L, \tag{6}$$

where

$$\sigma_k = \begin{cases} 0, & k = 1, \\ \sigma_t, & k = 2,3. \end{cases} \tag{7}$$

In further calculations, it was assumed that σ_t is equal to the material strength of the specimen determined in the Brazilian test (compressed disc without slot).

In further calculations, it was assumed that σ_t is equal to the material strength of the specimen determined in the Brazilian test (compressed disc without slot).

Fulfilling boundary condition Eq. (5) using potentials Eq. (4) we obtain the system of singular integral equations with unknown functions $g'_m(t)$ $(m = 1,2,3)$

$$\frac{1}{\pi}\sum_{k=1}^{3}\int_{L_k}\left[K_{km}(t,t')g'_m(t)dt + L_{km}(t,t')\overline{g'_m(t)}\,d\bar{t}\right] = p_m(t'), \quad t' \in L_m, \quad m = 1,2,3, \tag{8}$$

where kernels are as follows:

$$K(t,t') = f_1(t,t') + \overline{f_2(t,t')} + \frac{d\bar{t}'}{dt}\left[t'\overline{g_2(t,t')} + \overline{h_2(t,t')}\right],$$

$$L(t,t') = f_2(t,t') + \overline{f_1(t,t')} + \frac{d\bar{t}'}{dt}\left[t'\overline{g_1(t,t')} + \overline{h_1(t,t')}\right],$$

and

$$f_1(t,t') = \frac{1}{2}\left[\frac{1}{t-t'} + \frac{\bar{t}}{t'\bar{t}-R^2}\right],$$

$$f_2(t,t') = \frac{t'(t\bar{t}-R^2)(t'\bar{t}-2R^2)}{2R^2(t'\bar{t}-R^2)^2},$$

$$g_1(t,t') = \frac{1}{2}\left[\frac{1}{(t-t')^2} - \frac{\bar{t}^2}{(t'\bar{t}-R^2)^2}\right],$$

$$g_2(t,t') = \frac{R^2(t\bar{t}-R^2)}{(t'\bar{t}-R^2)^3},$$

$$h_1(t,t') = \frac{1}{2}\left[-\frac{\bar{t}}{(t-t')^2} + \frac{\bar{t}^3}{(t'\bar{t}-R^2)^2}\right],$$

$$h_2(t,t') = \frac{1}{2}\left\{\frac{1}{t-t'} + \frac{\bar{t}\left[4R^4-3R^2\bar{t}(t'+t)+t'\bar{t}^2(t'+t)\right]}{(t'\bar{t}-R^2)^3}\right\}.$$

3. NUMERICAL SOLUTION OF INTEGRAL SINGULAR EQUATIONS

We assume a clockwise direction of tracing the contour L_1 so the elastic region stays on the left during tracing. Taking into consideration the symmetry of the contour concerning both coordinate axes, we can write its parametric equation in the form [2]:

$$t = R\omega_1(\xi) = R\begin{cases}\omega_q(\xi), & 0 \le \xi < \pi/2, \\ -\overline{\omega_q(\pi-\xi)}, & \pi/2 \le \xi < \pi, \\ -\omega_q(\xi-\pi), & \pi \le \xi < 3\pi/2, \\ \overline{\omega_q(2\pi-\xi)}, & 3\pi/2 \le \xi < 2\pi. \end{cases} \tag{9}$$

Here, the function $\omega_q(\xi)$ describes the segment of contour L_1 laying in the fourth quarter of the coordinate system:

$$\omega_q(\xi) = \begin{cases} 1-\varepsilon_0+\varepsilon_0(\cos c\xi - i\sin c\xi), & 0 \le \xi < \pi/(2c), \\ \varepsilon_0 c(\pi/2-\xi) - i\varepsilon_0, & \pi/(2c) \le \xi \le \pi/2, \end{cases} \tag{10}$$

where parameter $c = 1 + 2(1/\varepsilon_0 - 1)/\pi$. Total curve L_1 length equals to $2\pi\varepsilon_0\gamma_0\, Rc$.

The parametric equation describing cut L_2 was written in the form

$$t = R\omega_2(\xi) = R\left[\gamma_0 + \frac{1}{2}(\gamma-\gamma_0)(1+\xi)\right], \ -1 \le \xi \le 1 \tag{11}$$

Contour L_3 is symmetrical to L_2 concerning the Oy axis so

$$t = R\omega_3(\xi) = -R\,\omega_2(\xi), \quad -1 \le \xi \le 1. \tag{12}$$

Introducing substitutions

$$\begin{aligned} &t = R\,\omega_1(\xi),\ \ t' = R\,\omega_1(\eta),\\ &t, t' \in L_1,\ \ 0 \le \xi,\ \eta \le 2\pi,\\ &t = R\,\omega_k(\xi),\ \ t' = R\,\omega_k(\eta),\\ &t, t' \in L_k,\ \ k = 2,3,\ -1 \le \xi, \eta \le 1, \end{aligned} \tag{13}$$

we reduce the system of integral equations Eq. (8) to the canonical form

$$\frac{1}{\pi}\int_0^{2\pi}\Big[M_{1m}(\xi,\eta)g_1'(\xi) + N_{1m}(\xi,\eta)\overline{g_1'(\xi)}\Big]\mathrm{d}\xi + \tag{14}$$

$$+\ \frac{1}{\pi}\sum_{k=2}^{3}\int_{-1}^{1}\Big[M_{km}(\xi,\eta)g_k'(\xi) + N_{km}(\xi,\eta)\overline{g_k'(\xi)}\Big]\mathrm{d}\xi = p_m(\eta), \qquad m = 1,2,3,$$

where

$$\begin{aligned} M_{km}(\xi,\eta) &= RK_{km}^*(R\omega_k(\xi), R\omega_m(\eta)),\\ N_{km}(\xi,\eta) &= RL_{km}^*(R\omega_k(\xi), R\omega_m(\eta)),\\ g_k'(\xi) &= g'(R\omega_k(\xi))\omega_k'(\xi),\\ p_m(\eta) &= p(R\omega_m(\eta)). \end{aligned}$$

The solution of the system of integral equations (14) consists of three complex functions $g'_k(\xi)$ assigned to the contours L_k. Function $g_1(\xi)$ $(0 \le \xi \le 2\pi)$ is 2π-periodic continuous function. However, in order to obtain a sufficiently accurate numerical solution, we have to densify quadrature nodes and collocation points in the vicinity of narrow slot tips. We use here a variant of sigmoid transformation [29,30] adapted to periodic case [29]:

$$\xi = G(\tau) = \tau - \frac{1}{2}\sin 2\tau, \qquad 0 \le \tau \le 2\pi. \tag{15}$$

Consequently, the function we are looking for is as follows

$$u_1(\tau) = g'_1(G(\tau)), \quad 0 \le \tau \le 2\pi. \tag{16}$$

A solution of the system of integral equations Eq. (14) for contours L_2 and L_3 is sought in the class of functions, which have an integrable singularity at the ends of the integration interval

$$g'_k(\xi) = \frac{u_k(\xi)}{\sqrt{1-\xi^2}}, \qquad -1 \le \xi \le 1, \tag{17}$$

where $u_k(\xi)$ $(k = 2,3)$ are continuous functions.

Finally, a modified system of the singular integral equations Eq. (14) takes the form

$$\frac{1}{\pi}\int_0^{2\pi}\Big[M_{1m}(\xi,\eta)u_1(\tau) + N_{1m}(\xi,\eta)\overline{u_1(\tau)}\Big]G(\tau)\mathrm{d}\tau + \tag{18}$$

$$+\ \frac{1}{\pi}\sum_{k=2}^{3}\int_{-1}^{1}\Big[M_{km}(\xi,\eta)u_k(\xi) + N_{km}(\xi,\eta)\overline{u_k(\xi)}\Big]\mathrm{d}\xi = p_m(\eta), \qquad m = 1,2,3,$$

In points $t = \pm\ell_0$ where contours L_2 and L_3 intersect contour L_1 the values of $g'_k(-1)$ $(k = 2,3)$ must be finite, thus we should provide two additional equations

$$u_k(-1) = 0, \qquad k = 2,3. \tag{19}$$

For numerical integration of the singular integral equation (18) two different methods must be used. For the closed-loop contour L_1, we apply the midpoint rule [31] and Gauss-Chebyshev quadrature [27] for L_2 and L_3 contours. Finally we get a system of complex linear algebraic equations which is the discrete analogue of the respective system of integral equations (18)

$$\frac{2}{n_1}\sum_{i=1}^{n_1}\Big[M_{1m}(\xi_i,\eta_j)u_1(\tau_i) + N_{1m}(\xi_i,\eta_j)\overline{u_1(\tau_i)}\Big]G(\tau_i) + \tag{20}$$

$$+\sum_{k=2}^{3}\left\{\frac{1}{n_k}\sum_{i=1}^{n_k}\Big[M_{km}(\xi_i,\eta_j)u_k(\xi_i) + N_{km}(\xi_i,\eta_j)\overline{u_k(\xi_i)}\Big]\right\} = p_m(\eta_j),$$

$$m = 1, \quad j = 1,\ldots,n_k,$$

$$m = 2,3, \quad j = 1,\ldots,(n_k - 1),$$

where quadrature nodes and collocation points are determined by formulas:

$$\begin{aligned} \xi_i &= G(\tau_i), \quad \tau_i = \frac{\pi(2i-1)}{n_1}, && i = 1,\ldots,n_1,\\ \eta_j &= G(\theta_j), \quad \theta_j = \frac{2\pi(j-1)}{n_1}, && j = 1,\ldots,n_1,\\ \xi_i &= \cos\frac{\pi(2i-1)}{2n_k}, && i = 1,\ldots,n_k, \quad k = 2,3,\\ \eta_j &= \cos\frac{\pi j}{n_k}, && j = 1,\ldots,(n_k-1), \quad k = 2,3. \end{aligned} \tag{21}$$

The linear system Eq. (20) consists of $n_1 + (n_2 - 1) + (n_3 - 1)$ complex equations. Using Lagrange interpolation on Chebyshev nodes [27] to conditions Eq. (19), we obtain two missing equations

$$\frac{1}{n_k}\sum_{i=1}^{n_k}(-1)^{i+n_k}\tan\frac{\pi(2i-1)}{4n_k}\,u_k(\xi_i) = 0, \qquad k = 2,3. \tag{22}$$

The right side of the Eq. (20) can be easily calculated using the relationship Eq. (6). Introducing the relationship $\lambda = \sigma_p/\sigma_t$ $(\sigma_p = P/(\pi R))$ as a relative load level parameter, we can write down $p_m(\eta_j)$ in compact form:

$$p_m(\eta_j) = \begin{cases} p_1(\eta_j), & m = 1,\\ \left(1 - \frac{1}{\lambda}\right)p_1(\eta_j), & m = 2,3, \end{cases} \tag{23}$$

where

$$p_1(\eta_j) = \sigma_p\frac{|\omega_k(\eta_j)|^2 - 1}{\overline{\omega_k(\eta_j)}^2 - 1}\left[\frac{2}{\overline{\omega_k(\eta_j)}^2 - 1}\frac{\overline{\omega_k'(\eta_j)}}{\omega_k'(\eta_j)} - \frac{|\omega_k(\eta_j)|^2 + 1}{\omega_k(\eta_j)^2 - 1}\right], \tag{24}$$

$k = 1,2,3.$

The solution to the problem is symmetrical concerning the axis Ox i Oy. The conditions resulting from symmetry concerning the sought function $u_k(\xi)$ and necessary kernel modifications are described in detail in Savruk et al. [32] (see also the literature [2]). Thus, the rank of the linear system Eq. (20) and (23) can be easily reduced by a factor of four.

The obtained values of sought function $u(\xi_k)$ fully determine the stress-strain state in the whole elastic region through an integral representation of complex stress potentials Eq. (4).

The slot edge (contour L_1) is free of applied loads, then the contour stress at the edge can be calculated using a simple formula [2].

$$\sigma_s = -4\sigma_p\,\Im\frac{u_1(\xi)}{\omega_1'(\xi)} = -4\sigma_p\,\Im\frac{u_1(\tau)}{\omega_1'(G(\tau))}. \tag{25}$$

Stress intensity factors in crack tips K_{I} and K_{II} can be directly expressed through the sought function $g'_k(t)$ Eq. (17). Let us introduce corresponding dimensionless stress intensity factors F_{I} and F_{II} using the following relationship

$$K_{\mathrm{I}}^+ - \mathrm{i}K_{\mathrm{II}}^+ = \left(F_{\mathrm{I}}^+ - \mathrm{i}F_{\mathrm{II}}^+\right)\sigma_p\sqrt{\pi R}. \tag{26}$$

DOI 10.2478/ama-2022-0047

Here upper indexes (+) indicate crack tip at $\xi = +1$. Taking into account relation Eq. (17), we get coefficients F_{I} and F_{II} [27]

$$F_{\mathrm{I}}^{+} - \mathrm{i}F_{\mathrm{II}}^{+} = -\sqrt{|\omega_{k'}(+1)|}\,\frac{u_k(+1)}{\omega_{k'}(+1)}, \quad k = 2,3, \tag{27}$$

where

$$u_k(+1) = -\frac{1}{n}\sum_{i=1}^{n_k}(-1)^i\, u_k(\xi_i)\cot\frac{\pi(2i-1)}{4n}, \quad k = 2,3. \tag{28}$$

Cracks L_2 and L_3 simulate fracture process zones (plastic strips) at the tips of narrow slot L_1, thus stresses at the crack L_k end must be finite

$$g'_k\left(t = \pm(\ell_0 + \ell)\right) = g'_k\left(R\omega_k(+1)\right) = 0, \quad \rightarrow$$
$$u_k(+1) = 0, \quad k = 2,3. \tag{29}$$

This condition allows us to calculate the unknown length $\ell = (\gamma - \gamma_0)R$ using a simple iteration process.

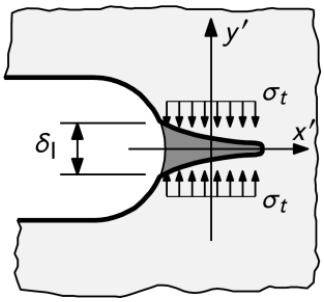

Fig. 2. U-notch tip opening displacement

The opening displacement in the notch tip (Fig. 2) can be calculated based on the known [27] relationship between function $g_k(t)$ $(k = 2,3)$ and displacement discontinuity $(v_k^+ - v_k^-)$ across the contour L_k

$$2G\,\frac{\mathrm{d}}{\mathrm{d}x'}(v_k^+ - v_k^-) = (1+\kappa)g'_k(x'),$$
$$x' \in L_k, \quad k = 2,3, \tag{30}$$

where x' is a local abscissa at contour L_k, G – shear modulus, κ – Muskhelishvili's constant.

In plane stress state $(1+\kappa)/(4G) = 2/E$, so we come to the formula for crack opening displacement in its left tip $x' = l_k^-$ $(x = \pm\ell_0)$, i.e. in slot tips, in the form [32]

$$\delta_{\mathrm{I}} = \delta_{\mathrm{I}}(l_k^-) = \frac{4}{E}\Re g_k(l_k^-) = -\frac{4}{E}\Re\int_{l_k^-}^{l_k^+} g'_k(t)\mathrm{d}t =$$
$$= -\frac{4R\sigma_p}{E}\Re\int_{-1}^{+1}\frac{u_k(\xi)}{\sqrt{1-\xi^2}}\mathrm{d}\xi = \tag{31}$$
$$= -\frac{\sigma_p R}{E}\frac{4\pi}{n_k}\sum_{i=1}^{n_k}\Re u_k(\xi_i), \quad k = 2,3.$$

4. NUMRICAL RESULTS

The calculations were performed for the constant rounding radius of slot tips $\rho_0 = 1/75\ R$. Relative slot span γ_0 was chosen from the set $\gamma_0 = \{0.1, 0.2, 0.3, 0.4, 0.5, 0.6\}$, so the relative rounding radius of the slot vertices can be easily calculated as $\varepsilon_0 = 1/(75\gamma_0)$. For every slot geometry and for arbitrary load level $\lambda = \sigma_p/\sigma_t$ $(\lambda_{\min} < \lambda < 1)$ the plastic strips range $\gamma = (\ell_0 + \ell)/R$ and notch tip opening displacement δ_{I} were calculated. These values are presented in Figs 3 and 4 respectively.

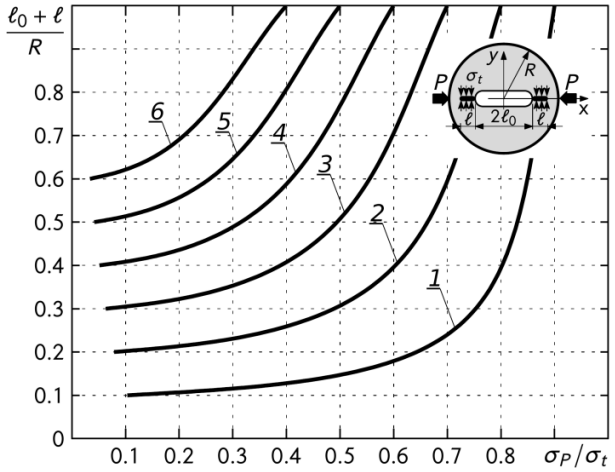

Fig. 3. Relative plastic strips range versus relative load level for the following relative slot span: 1 – 0.1, 2 – 0.2, 3 – 0.3, 4 – 0.4, 5 – 0.5, 6 – 0.6

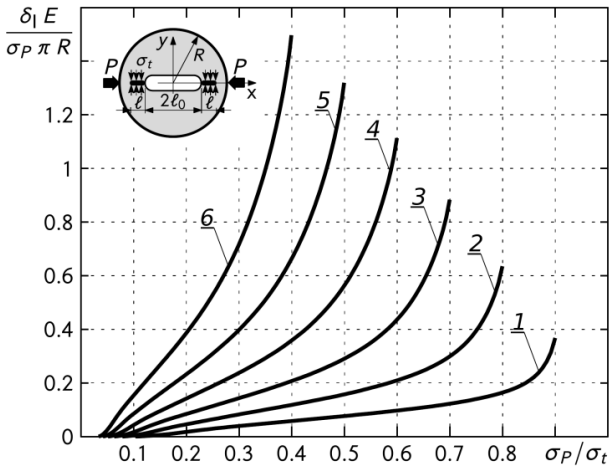

Fig. 4. Dimensionless notch tip opening displacement versus relative load level for the following relative slot spa:n1 – 0.1, 2 – 0.2, 3 – 0.3, 4 – 0.4, 5 – 0.5, 6 – 0.6

As it can be easily seen, the values of relative load level λ start with a certain value $\lambda_{\min}$. Plastic strips arise when the maximum normal stress $\sigma_{\max}$ at the vertex of the narrow slot reaches the limit value σ_t. If we denote the stress concentration factor in the rounded notch tip as k, then $k\sigma_p = \sigma_{\max} \le \sigma_t$ and the minimum value of the load level parameter will be equal to $\lambda_{\min} = 1/k$. Stress concentration factor can be easily calculated (see Savruk and Kazberuk [2]) by solving the system of equations (20) taking into account contour L_1 only and then using Eq. (26). A list of the stress concentration factors for all γ_0 values used here is shown in Tab. 1.

When the plastic deformations are small, the critical stress intensity factor K_c can be calculated with the formula [1,33]

$$K_c = \sqrt{\delta_{\mathrm{I}}\,E\sigma_t} = \sqrt{\tilde{\delta}_{\mathrm{I}}\,\lambda}\ \sigma_t\sqrt{\pi\,R}. \tag{32}$$

Tab. 1. Stress concentrations factors at the rounded vertex of narrow slot and dimensionless stress intensity factors at the tips of a corresponding central crack in disc specimen

$\gamma_0 = \frac{\ell_0}{R}$	$\varepsilon_0 = \frac{\rho}{\ell_0}$	$k = \frac{\sigma_{\max}}{\sigma_p}$	$F_{\mathrm{I}} = \frac{K_{\mathrm{I}}}{\sigma_p \sqrt{\pi R}}$
0.1	0.1333	9.685	0.3210
0.2	0.0667	12.75	0.4741
0.3	0.0444	15.89	0.6220
0.4	0.0333	19.54	0.7866
0.5	0.0267	24.04	0.9838
0.6	0.0222	29.90	1.2364

Let's compare the obtained results with the approximate estimation calculated for a semi-infinite U-notch [25]. The relative load level parameter is equal

$$\gamma^{\infty} = \frac{1}{\sqrt{2\pi\rho}} \frac{K_{\mathrm{I}}}{\sigma_t} = \frac{F_{\mathrm{I}}}{\sqrt{2\varepsilon_0\gamma_0}} \frac{1}{\sigma_t} \frac{P}{\pi R} = \frac{F_{\mathrm{I}}}{\sqrt{2\varepsilon_0\gamma_0}} \lambda, \tag{33}$$

Dimensionless notch opening displacement is equal [25]

$$\sqrt{\tilde{\delta}_{\mathrm{I}}^{\infty}} = 1 - \frac{1}{R_{\mathrm{I}}^2 (\gamma^{\infty})^2}, \tag{34}$$

where the stress rounding factor [34] is equal $R_{\mathrm{I}} = 2.993$ [35].

The value of the critical stress intensity factor, calculated based on the criteria condition Eq. (32), is equal

$$K_c^{\infty} = \sqrt{\tilde{\delta}_{\mathrm{I}}^{\infty}}\, K_{\mathrm{I}} = F_{\mathrm{I}}\, \lambda \sigma_t \sqrt{\tilde{\delta}_{\mathrm{I}}^{\infty}\, \pi\, R}, \tag{35}$$

where dimensionless stress intensity factors F_{I} are shown in Tab 1.

In Fig. 5. the comparison of the values of the critical stress intensity factors calculated for the notched disk Eq. (33) and for semi-finite U-notch in the tensile plane Eq. (36) is shown. It can be seen that coarse approximation is only valid for the smallest slot $(\gamma_0 = 0.1)$ under load level $0.4 < \lambda < 0.8$. For relative slot span $\gamma_0 = 0.2$ differences between exact and approximated values are much greater – nearly 30% at $\lambda \sim 0.5$.

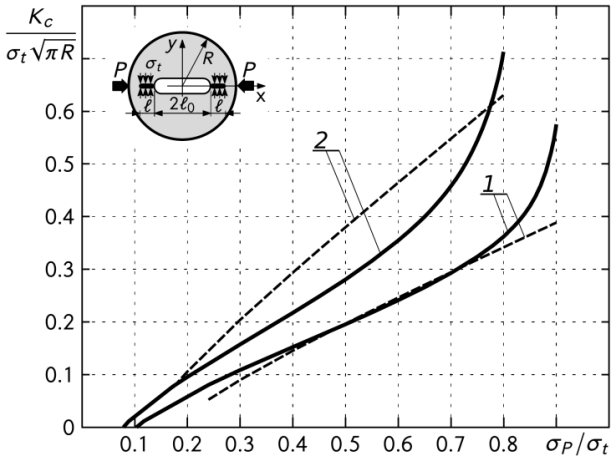

Fig. 5. Comparison of the values of the critical stress intensity factors calculated for notched disc (solid lines) and at the vertex of the semi-infinite U-notch (dashed lines) as a function of the relative load level for the following parameters: $1 - \gamma_0 = 0.1, 2 - \gamma_0 = 0.2$

5. CONCLUSIONS

The elastic-plastic problem for the Brazilian disc with a central narrow slot in the plane stress state condition was solved. The solution was obtained by the method of singular integral equations using complex stress potentials for a system of cracks and openings in the two-dimensional circular elastic domain. All necessary analytical background was documented in detail. Based on the Dugdale model of fracture process zone and deformation fracture criterion, the relationships between critical load, notch tip opening displacement and length of the plastic strips were established. Numerical calculations for arbitrary but representative sets of geometrical parameters were performed. The correctness of the solution was checked by comparing the results with the approximate relationships obtained for the problem of semi-infinite U-notch in an elastic plane subjected to unidirectional tension. For a small relative slot span, both results are in good agreement.

The presented approach, despite the obvious simplifications resulting from the adopted assumptions (plane stress state, fracture process zone as a plastic strip), can be used to estimate the fracture mechanics parameters of quasi-brittle materials determined in the Brazilian test.

REFERENCES

1. Rice JR. Limitations to the small scale yielding approximation for crack tip plasticity. J Mech Phys Solids. 1974;22(1):17-26.
2. Savruk MP, Kazberuk A. Stress Concentration at Notches. Springer International Publishing Switzerland; 2017.
3. Li D, Wong LNY. The Brazilian disc test for rock mechanics applications: review and new insights. Rock mechanics and rock engineering. 2013;46(2):269-87.
4. Garcıa VJ, Marquez CO, Zuniga-Suarez AR, Zuniga-Torres BC, VillaltaGranda LJ. Brazilian Test of Concrete Specimens Subjected to Different Loading Geometries: Review and New Insights. International Journal of Concrete Structures and Materials. 2017;11(2):343-63.
5. Libatskii L, Kovchik S. Fracture of discs containing cracks. Mater Sci. 1967;3(4):334-9.
6. Yarema SY, Krestin GS. Determination of the modulus of cohesion of brittle materials by compressive tests on disc specimens containing cracks. Mater Sci. 1967;2(1):7-10.
7. Yarema SY, Krestin GS. Limiting equilibrium of a disk with a diametral crack. Int Appl Mech. 1968;4(7):55-8.
8. Yarema SY. Stress state of disks with cracks, recommended as specimens for investigating the resistance of materials to crack development. Mater Sci. 1977;12(4):361-74.
9. Yarema SY, Ivanitskaya G, Maistrenko A, Zboromirskii A. Crack development in a sintered carbide in combined deformation of types I and II. Strength of Materials. 1984;16(8):1121-8.
10. Atkinson C, Smelser R, Sanchez J. Combined mode fracture via the cracked Brazilian disk test. Int J Fract. 1982;18(4):279-91.
11. Awaji H, Sato S. Combined mode fracture toughness measurement by the disk test. J Eng Mater Technol. 1978;100:175-82.
12. Zhou S. Fracture Propagation in Brazilian Discs with Multiple Pre-existing Notches by Using a Phase Field Method. Periodica Polytechnica Civil Engineering. 2018;62(3):700-8.
13. Xiankai B, Meng T, Jinchang Z. Study of mixed mode fracture toughness and fracture trajectories in gypsum interlayers in corrosive environment. Royal Society Open Science. 2018;5(1).
14. Tang SB. Stress intensity factors for a Brazilian disc with a central crack subjected to compression. International Journal of Rock Mechanics and Mining Sciences. 2017;93:38 45.

15. Seitl S, Miarka P. Evaluation of mixed mode I/II fracture toughness of C 50/60 from Brazilian disc test. Frattura ed Integrità Strutturale. 2017;11(42):119-27.
16. Ayatollahi MR, Aliha MRM. On the use of Brazilian disc specimen for calculating mixed mode I–II fracture toughness of rock materials. Engineering Fracture Mechanics. 2008;75(16):4631 4641.
17. Ayatollahi MR, Aliha MRM. Wide range data for crack tip parameters in two disc-type specimens under mixed mode loading. Computational Materials Science. 2007;38(4):660 670.
18. Atahan HN, Tasdemir MA, Tasemir C, Ozyurt N, Akyuz S. Mode I and mixed mode fracture studies in brittle materials using the Brazilian disc specimen. Mater Struct. 2005;38:305-12.
19. Dong S. Theoretical analysis of the effects of relative crack length and loading angle on the experimental results for cracked Brazilian disk testing. Engineering Fracture Mechanics. 2008;75(8):2575 2581.
20. Wang QZ, Gou XP, Fan H. The minimum dimensionless stress intensity factor and its upper bound for CCNBD fracture toughness specimen analyzed with straight through crack assumption. Engineering Fracture Mechanics. 2012;82:1 8.
21. Ayatollahi MR, Aliha MRM. Mixed mode fracture in soda lime glass analyzed by using the generalized MTS criterion. International Journal of Solids and Structures. 2009;46(2):311 321.
22. Savruk MP, Kazberuk A. Problems of fracture mechanics of solid bodies with V-shaped notches. Mater Sci. 2009;45(2):162-80.
23. Leonov MY, Panasyuk VV. Development of a nanocrack in a solid. Prikl Mekh. 1959;5(4):391-401.
24. Dugdale D. Yielding of steel sheets containing slits. J Mech Phys Solids. 1960;8:100-4.
25. Kosior-Kazberuk M, Kazberuk A, Bernatowicz A. Estimation of Cement Composites Fracture Parameters Using Deformation Criterion. Materials. 2019;12(24):4206.
26. Panasyuk VV, Savruk MP. Model for plasticity bands in elastoplastic failure mechanics. Mater Sci. 1992;28(1):41-57.
27. Savruk MP. Two-dimensional problems of elasticity for bodies with cracks (in Russian). Naukova Dumka, Kiev; 1981.
28. Muskhelishvili NI. Some Basic Problems of the Mathematical Theory of Elasticity. 2nd ed. Noordhoff International Publishing, Leyden; 1977.
29. Sidi A. A new variable transformation for numerical integration. H Brass H and G Hammerlin, editors, Numerical integration IV. 1993:359-73.
30. Johnston PR. Application of sigmoidal transformations to weakly singular and near-singular boundary element integrals. Int J Numer Meth Eng. 1999;45:1333-48.
31. Belotserkovsky SM, Lifanov IK. Method of discrete vortices. CRC Press LLC, Boca Raton; 1993.
32. Savruk MP, Osiv PN, Prokopchuk IV. Numerical analysis in plane problems of the crack theory (in Russian). Naukova Dumka, Kiev; 1989.
33. Rice JR. The location of plastic deformation. Theor Appl Mech. 1976;1:20720.
34. Benthem JP. Stresses in the region of rounded corners. Int J Solids Struct. 1987;23(2):239-52.
35. Savruk MP, Kazberuk A. Relationship between the stress intensity and stress concentration factors for sharp and rounded notches. Mater Sci. 2006;42(6):725-38.

The work has been accomplished under the research project No. WZ/WM-IIM/3/2020.

Andrzej Kazberuk: https://orcid.org/0000-0003-4179-0312